World Journal of Stem Cells

Submit a Manuscript: https://www.f6publishing.com

World J Stem Cells 2023 May 26; 15(5): 476-489

DOI: 10.4252/wjsc.v15.i5.476

ISSN 1948-0210 (online)

ORIGINAL ARTICLE

Basic Study

Exosomes from circ-Astn1-modified adipose-derived mesenchymal stem cells enhance wound healing through miR-138-5p/SIRT1/FOXO1 axis regulation

Zhi Wang, Cheng Feng, Hao Liu, Tian Meng, Wei-Qing Huang, Ke-Xin Song, You-Bin Wang

Specialty type: Cell and tissue engineering

Provenance and peer review: Unsolicited article; Externally peer reviewed.

Peer-review model: Single blind

Peer-review report's scientific quality classification

Grade A (Excellent): A
Grade B (Very good): B, B
Grade C (Good): C
Grade D (Fair): 0
Grade E (Poor): 0

P-Reviewer: Amin A, United Arab Emirates; Morya AK, India; Qin Y, China; Li SC, United States

Received: June 13, 2022
Peer-review started: June 13, 2022
First decision: June 23, 2022
Revised: July 5, 2022
Accepted: September 9, 2022
Article in press: September 9, 2022
Published online: May 26, 2023

Zhi Wang, Cheng Feng, Hao Liu, Tian Meng, Wei-Qing Huang, Ke-Xin Song, You-Bin Wang, Department of Plastic and Cosmetic Surgery, Peking Union Medical College Hospital, Beijing 100730, China

Corresponding author: Zhi Wang, MD, Doctor, Department of Plastic and Cosmetic Surgery, Peking Union Medical College Hospital, No. 1 Shuaifuyuan, Dongcheng District, Beijing 100730, China. wangzh@pumch.cn

Abstract

BACKGROUND

Wound healing impairment is a dysfunction induced by hyperglycemia and its effect on endothelial precursor cells (EPCs) in type 2 diabetes mellitus. There is increasing evidence showing that exosomes (Exos) derived from adipose-derived mesenchymal stem cells (ADSCs) exhibit the potential to improve endothelial cell function along with wound healing. However, the potential therapeutic mechanism by which ADSC Exos contribute to wound healing in diabetic mice remains unclear.

AIM

To reveal the potential therapeutic mechanism of ADSC Exos in wound healing in diabetic mice.

METHODS

Exos from ADSCs and fibroblasts were used for high-throughput RNA sequencing (RNA-Seq). ADSC-Exo-mediated healing of full-thickness skin wounds in a diabetic mouse model was investigated. We employed EPCs to investigate the therapeutic function of Exos in cell damage and dysfunction caused by high glucose (HG). We utilized a luciferase reporter (LR) assay to analyze interactions among circular RNA astrotactin 1 (circ-Astn1), sirtuin (SIRT) and miR-138-5p. A diabetic mouse model was used to verify the therapeutic effect of circ-Astn1 on Exo-mediated wound healing.

RESULTS

High-throughput RNA-Seq analysis showed that circ-Astn1 expression was increased in ADSC Exos compared with Exos from fibroblasts. Exos containing high concentrations of circ-Astn1 had enhanced therapeutic effects in restoring

EPC function under HG conditions by promoting SIRT1 expression. Circ-Astn1 expression enhanced SIRT1 expression through miR-138-5p adsorption, which was validated by the LR assay along with bioinformatics analyses. Exos containing high concentrations of circ-Astn1 had better therapeutic effects on wound healing *in vivo* compared to wild-type ADSC Exos. Immunofluorescence and immunohistochemical investigations suggested that circ-Astn1 enhanced angiopoiesis through Exo treatment of wounded skin as well as by suppressing apoptosis through promotion of SIRT1 and decreased forkhead box O1 expression.

CONCLUSION

Circ-Astn1 promotes the therapeutic effect of ADSC-Exos and thus improves wound healing in diabetes *via* miR-138-5p absorption and SIRT1 upregulation. Based on our data, we advocate targeting the circ-Astn1/miR-138-5p/SIRT1 axis as a potential therapeutic option for the treatment of diabetic ulcers.

Key Words: Adipose-derived mesenchymal stem cells; Circular RNA astrotactin 1; Diabetic; Exosomes; Angiogenesis

Core Tip: Circular RNA astrotactin 1 (circ-Astn1) promoted the therapeutic effect of adipose-derived mesenchymal stem cells-exosomes and thus improved wound healing in diabetes *via* miR-138-5p absorption and SIRT1 upregulation. Based on our data, we advocate targeting the circ-Astn1/miR-138-5p/SIRT1 axis as a potential therapeutic alternative for diabetic ulcers.

Citation: Wang Z, Feng C, Liu H, Meng T, Huang WQ, Song KX, Wang YB. Exosomes from circ-Astn1-modified adipose-derived mesenchymal stem cells enhance wound healing through miR-138-5p/SIRT1/FOXO1 axis regulation. *World J Stem Cells* 2023; 15(5): 476-489
URL: https://www.wjgnet.com/1948-0210/full/v15/i5/476.htm
DOI: https://dx.doi.org/10.4252/wjsc.v15.i5.476

INTRODUCTION

Diabetes affects 30 million children as well as adults in the United States, *i.e.* one out of every eleven people in the United States, which leads to $327 billion costs each year. Consequently, it is important to develop a new method of diabetes treatment. Interventions that improve healing rates and decrease diabetic ulcer size could lower the infection incidence, amputation rate, and care cost[1]. Diabetic foot (DF) is a severe complication of type 2 diabetes mellitus (T2D). DF infection is the main reason for DF development and deterioration, and controlling infection plays an important role in disease treatment. Previous studies have found that diabetes is associated with hyperglycemia, one of the most important causes of oxidative stress. Endogenous antioxidants are able to destroy the reactive species and create a balance between antioxidants and free radicals[2,3]. The impaired function and senescence of endothelial progenitor cells (EPCs) and high glucose (HG)-induced reactive oxygen species likely exacerbate DFs[4].

Accumulated evidence shows that mesenchymal stem cell (MSC)transplantation promotes angiogenesis and accelerates diabetic wound healing[5,6]. Adipose-derived mesenchymal stem cells (ADSCs) therapy provides potentially new therapeutic options to improve diabetic wound healing[7], and autologous stem cell transplantation reduces the cost of drug development, which in turn reduces financial costs. However, the mechanism is not clear.

Stem cells live in niches, which are complicated microenvironments that exert important functions in directing the division, differentiation, and activity of stem cells. However the direction of differentiation is affected by hypoxia, cytokines, trophic factors, chemical and pharmacological agents, and physical factors[8]. Considering the safety of *in vivo* transplantation, some investigations have suggested that exosomes (Exos) from ADSCs play a similar functional role to ADSCs in promoting diabetic wound healing. Exos are tiny endosomal membrane-bound vesicles, 50–200 nm in length, that have a variety of contents including protein and nucleic acids which vary with cell or tissue origin. They play their full role by fusing with selected cells and releasing their cargo that could contain bioactive molecules including lipids, proteins, non-coding-RNA (ncRNA)[9-11] and mRNAs. Previous studies have found that Exos can regulate the epithelial–mesenchymal transition and disease progression in different cancers[12,13]. Exos secreted from ADSCs attenuate diabetic nephropathy by promoting autophagy flux

and by inhibiting apoptosis in podocytes[14]. Exos from nuclear factor erythroid 2–related factor 2-overexpressing ADSCs accelerate cutaneous wound healing by promoting vascularization in a DF ulcer [4]. Exos from linc00511-overexpressing ADSCs accelerate angiogenesis in healing DF ulcers by suppressing progestin and adipoQ receptor family member 3-induced Twist1 degradation[15]. However, it remains largely unknown if Exos from ncRNA-modified ADSCs can improve wound healing.

The ncRNAs include circular RNA (circRNA), long non-coding RNA (lncRNA), and microRNA (miRNA). circRNA activity is indispensable during the regulation of gene expression, demonstrating that circRNAs function not only as candidate therapeutic agents but also as diagnostic markers. circRNA 5′ and 3′ extremities are linked to form an integrated circular structure, which makes circRNAs more resistant to RNA exonuclease degradation. as well as more stable 8than linear RNAs[16,17]. A previous study found that circRNAs possess activity and potential clinical benefits in skin wound healing[18].

To identify relevant circRNAs as therapeutic targets, we used high-throughput sequencing detection to identify the function of mmu_circ_0000101 (circ-Astn1), which acts as the key factor in delivery by ADSC Exos. Exos from circ-Astn1-modified ADSCs improve wound repair in diabetic rats through miR-138-5p/SIRT1 pathway regulation. The present study verified the effect of treatment with Exos from circ-Astn1-overexpressing ADSCs on HG-induced EPC dysfunction. The abundance and simple methods of sampling of ADSC-Exos make it safer in terms of trauma and other adverse reactions.

MATERIALS AND METHODS

Ethics statement

The Animal Care and Use Committee of Peking Union Medical College Hospital approved the investigation protocol (No: XHDW-2020-01; Beijing, China). We carried out all postoperative animal care along with surgical interventions following the National Institutes of Health Guidelines for the Care and Use of Laboratory Animals. All surgeries and euthanasia were performed under sodium pentobarbital anesthesia (30 mg/kg) by intraperitoneal injection, and all efforts were made to minimize suffering.

High-throughput and strand-specific RNA sequencing library construction

Total RNA from ADSCs and fibroblast Exos was isolated using TRIzol reagent (Invitrogen, Carlsbad, CA, United States). Our team prepared about 3 μg total RNA *per* sample using the VAHTS Total RNA-seq (H/M/R) Library Prep Kit from Illumina (Vazyme Biotech Co., Ltd., Nanjing, China) to isolate the ribosomal RNA and remove other RNAs such as ncRNA and mRNA. We then performed RNA purification using RNase R (Epicenter, 40 U, 37 °C for 3 h) followed by TRIzol. An RNA sequencing RNA-Seq) library was prepared using the KAPA Stranded RNA-Seq Library Prep Kit (Roche, Basel, Switzerland) and they were exposed in order following extensive codifying with Illumina HiSeq 4000 from Aksomics, Inc. (Shanghai, China).

Cell treatment

To investigate endothelial precursor cell (EPC) dysfunction as well as apoptosis, we cultivated EPCs at 37 °C with 5% carbon dioxide in EPC medium (Gibco, Carlsbad, CA, United States) and processed them after 1 d using 5.5 or 30 mmol/L glucose. We harvested EPCs for detection of apoptosis as well as to test their response to Exo therapy. In order to study the protective function of Exos on EPCs, we added 100 μg/mL Exos to cultures following 80% EPC fusion to evaluate the protective function against damage caused by prior HG treatment with various glucose concentrations.

ADSC isolation and identification

We isolated ADSCs from adipose tissue following the method used in a previous study[4]. We observed no uninduced differentiation in cultural expansion. We induced osteogenic differentiation *via* a 3-wk culture of ADSCs in Dulbecco's Modified Eagle Medium (DMEM) supplemented with 10% fetal bovine serum (FBS), 0.1 μM dexamethasone, 50 μM ascorbate-2-phosphate, and 10 mmol/L β-glycerophosphate. We induced adipogenic differentiation through culturing ADSCs for 2 weeks in DMEM supplemented with 10% FBS, 10 μM insulin, 0.5 mmol/L isobutylmethylxanthine, 200 μM indomethacin, and 1 μM dexamethasone. We also investigated the osteogenic or adipogenic differentiation of ADSCs through Oil-Red O and alkaline phosphatase staining.

Identification and isolation of ADSC-derived Exos

We isolated ADSC-derived Exos when cells reached 80%-90% confluence. Our team rinsed ADSCs from various groups with phosphate-buffered saline (PBS), and then cultured them in FBS-free endothelial cell growth medium (EGM)-2MV, which was supplemented with 1 × serum replacement solution (PeproTech, Rocky Hill, NJ, United States) for another 2 d. Then, we collected conditioned culture medium and centrifuged it at 300 × *g* for 10 min to remove cells and at 2000 × *g* for another 10 min to

remove apoptotic cells and cellular debris. Following centrifugation at 10000 × *g* for 30 min, we filtered the supernatant through a 0.22 μm filter (Millipore, Billerica, MA, United States), then transferred 15 mL supernatant to the Amicon Ultra-15 Centrifugal Filter Unit (100 kDa) and centrifuged it at 4000 × *g* to concentrate to approximately 1 mL. The ultrafiltration unit was washed twice with PBS centrifuged it again at 100000 × *g*, and the supernatant was aspirated. All processes were conducted at 4 °C. We resuspended the Exo pellets obtained in 500 μL PBS. Finally, the Exo protein content was evaluated using the Pierce bicinchoninic acid assay (BCA) Protein Assay Kit (Thermo Fisher Scientific, Waltham, MA, United States). We stored Exos at -80 °C until subsequent use for experiments and identified Exos by western blotting and transmission electron microscopy.

Diabetic wound induction

We utilized Balb/c mice and induced diabetes through a single intraperitoneal injection of 60 mg/kg streptozotocin (STZ) dissolved in 0.1 M citrate buffer (pH 4.5). Three days after STZ administration, we confirmed diabetes development by measuring fasting blood glucose levels in blood samples obtained from the tail vein. We considered a mouse with fasting blood glucose levels > 250 mg/dL diabetic, which we maintained for 1 mo and employed for subsequent analyses of posterior blood glucose stabilization. Following diabetes validation, we anesthetized mice through intramuscular injection with ketamine hydrochloride and xylazine cocktail at 80 and 10 mg/kg, respectively. Once anesthesia was established, hair was shaved from the dorsal leg area and the region was sterilized using povidone iodine solution. A sterile biopsy punch was used to generate a full-thickness 4 mm excisional wound. Then we allocated mice randomly to subcutaneous injection with 100 μL PBS containing 200 μg ADSC Exos or equivalent amount of PBS without Exos at four sites near the wound (25 μL/site). We euthanized mice and harvested skin specimens for histopathological validation.

RNA overexpression or interference

RNA overexpression or interference was induced by transfection of miR-138-5p mimics or inhibitor, circ-Astn1 and SIRT1 overexpression vector, and siRNA against circ-Astn1 (si-circ-Astn1) obtained from RiboBio (Guangzhou, China). Our team performed transfection using Lipofectamine 2000 (Thermo Fisher Scientific) following a method previously described[19].

Quantitative polymerase chain reaction

We isolated total RNA from skin tissue or cells from wounds using a TRIzol reagent kit. Our team synthesized cDNA to amplify with TaqMan miRNA Reverse Transcription Kit. Our team then performed quantitative polymerase chain reaction (qPCR) using a TaqMan Human miRNA Assay Kit, using the $2^{-\Delta\Delta CT}$ approach to detect fold changes with respect to expression. We used *U6* and glyceraldehyde-3-phosphate dehydrogenase (*GAPDH*) as internal references. Primers utilized were: Circ-Astn1, F: 5′-CTGGACCCTTGTGAACACCAATG-3′, R, 5′-GGATCATCACCAGGCACAAGATG-3′; FOXO1, F: 5′-AAGGCCATCGAGAGCTCAGC-3′, R, 5′-GATTTTCCGCTCTTGCCTCC-3′; miR-138-5p, F: 5′-GCTGGTGTTGTGAATCAG-3′, R: 5′-GAACATGTCTGCGTATCTC-3; U6, F: 5′-AGTAAGCCCTTGCTGTCAGTG-3′, R: 5′-CCTGGGTCTGATAATGCTGGG-3′; GAPDH: F: 5′-GTCTCCTCTGACTTCAACAGCG-3′, R: 5′-ACCACCCTGTTGCTGTAGCCAA-3′, and were designed by Gene Pharma (Shanghai, China).

Apoptosis detection

To assess apoptosis, we collected cells into centrifuge tubes and centrifuged them at 1000 rpm for 5 min. We resuspended cells in PBS at 4 °C and removed the supernatant following centrifugation. We resuspended the cell pellet at 1–5 × 10^6/mL in 1 × binding buffer, then 100 μL cell suspension was mixed with 5 μL Annexin V/fluorescein isothiocyanate in the dark at room temperature for 5 min. Lastly, we added 10 μL propidium iodide (PI) and 400 μL PBS to stain the cells. We analyzed data using the FlowJo package.

Immunofluorescence and immunohistochemical assays

We fixed skin tissue samples in 10% formalin solution, embedded them in paraffin, and sectioned them at 5 μm. Our team stained tissue sections with hematoxylin and eosin (HE) for histological detection, and cluster of differentiation 31 (CD31) immunofluorescence staining was used to detect histopathological changes associated with angiogenesis. We performed terminal deoxynucleotidyl transferase dUTP nick end labeling (TUNEL) to identify apoptotic cells. Our team visualized sections using fluorescence (Nikon, Tokyo, Japan) or light microscope (Zeiss, Oberkochen, Germany), and photographed them using a digital camera.

Western blot analysis

Skin tissues were lysed, and lysates were centrifuged at 12000 rpm at 4 °C following addition of a protease inhibitor. The protein concentration was determined using the Pierce BCA kit (Thermo Fisher). Proteins were separated by 10% sodium dodecyl sulfate-polyacrylamide gel electrophoresis and electrotransferred to PVDF membranes. The primary antibodies used to assay protein expression were SIRT1

(1:600), forkhead box O1 (FOXO1) (1:600) (all from Santa Cruz Biotechnology, Santa Cruz, CA, United States), and anti-GAPDH (1:1000; Sigma-Aldrich, St. Louis, MO, United States), followed by a horseradish peroxidase-conjugated secondary antibody (1:1000; Abcam, Cambridge, MA, United States). An enhanced chemiluminescence kit (Millipore, Burlington, MA, United States) was used to read the bands.

Luciferase reporter assay

We created and cloned wild-type (WT) and 3'-UTR mutant (MUT) *SIRT1*, as well as WT and MUT *circ-Astn1* into pMIR firefly luciferase-expressing vectors. We co-transfected the vectors into HEK293T cells once they reached 70% confluence, using 500 ng pMIR-SIRT1-wt/pMIR-SIRT1-Mut or pMIR-*circ-Astn1*-wt/pMIR-*circ-Astn1*-Mut combined with 50 nM miR-138-5p mimics using a Lipofectamine 2000 Transfection Kit for the luciferase assay. We assayed luciferase activity using a Dual-Luciferase Reporter System (Promega, Madison, WI, United States). We performed five independent assays.

Tube formation assay

We performed an EPC tube formation assay using Matrigel (BD Biosciences, Franklin Lakes, NJ, United States). Matrigel solution was mixed with ECMatrix diluent buffer then spread on μ-Slide plates and incubated at 37 °C for 1 h for the matrix solution to solidify. Next, we added various treatments to the EPCs (2×10^4 cells/well) to wells containing solid matrix and cultured them with EGM-2 medium at 37 °C for a period of 12 h. Our team detected tube formation under an inverted light microscope (100 ×) and evaluated three independent representative fields from each well to determine mean tube number.

Cell Counting Kit (CCK)-8 assay

EPC proliferation was evaluated using the Cell Counting Kit-8 (CCK-8) (BD Biosciences). Our team cultivated transfected cells in 96-well plates with Exos in HG conditions for 1 d in wells to which 10 μL CCK-8 reagent and 90 μL fresh culture medium was previously added. Absorbance was detected at 450 nm using a microplate reader following incubation at 37 °C for 2 h.

Statistical analyses

We denoted continuous parameters by the mean ± SD and employed one-way variance of analysis (ANOVA) to compare data using GraphPad Prism (GraphPad, La Jolla, CA, United States). $P \leq 0.05$ indicated a statistically significant difference.

RESULTS

ADSC and Exo characterization

Isolated ADSCs have classical cobblestone-like morphology (Figure 1A). Immunofluorescence staining showed that ADSCs from mouse adipose tissue samples were positive for expression of the mesenchymal cell surface markers CD29 (Figure 1B), CD44 (Figure 1C), CD90 (Figure 1D), and CD105 (Figure 1E), but negative for expression of the endothelial cell marker CD31 (Figure 1F) as well as von Willebrand Factor (Figure 1G). The results of Oil Red O staining (Figure 1H) together with alkaline phosphatase staining (Figure 1I) verified that isolated ADSCs possessed both osteoblastic and adipocytic differentiation capacity. We concluded that ADSCs have the potential for multidirectional differentiation[20].

Exos were isolated by ultra-high-speed centrifugation. Transmission electron microscopy revealed that ADSC Exos had spherical or cup-shaped morphology with a diameter ranging from 50 to 120 nm (Figure 1J) as previously reported[21]. Western blotting suggested that ADSC Exos were positive for the Exo markers CD81 and CD63, which are cellular components (Figure 1K).

Exos derived from circ-Astn1-modified ADSCs play important roles in the restoration of EPC function by decreasing apoptosis under HG conditions

To determine the role of circRNAs in ADSC Exo-mediated restoration of EPC function under HG conditions, circRNA expression in ADSCs and fibroblast Exos was explored by RNA-Seq. The results verified that the contents of mmu_circ_0000101, mmu_circ_0008040, mmu_circ_0008061, and mmu_circ_0008099 were all significantly upregulated in ADSC Exos compared with fibroblast Exos (Figure 2A). RT-qPCR analysis confirmed that mmu_circ_0000101, mmu_circ_0008040, mmu_circ_0008061 and mmu_circ_0008099 expression in EPCs decreased after exposure to HG conditions (Figure 2B), with expression of mmu_circ_0000101 in particular decreasing most significantly. Consequently, mmu_circ_0000101 was selected for subsequent study. Mmu_circ_0000101 originated from *Astn1* gene exon 5, so mmu_circ_0000101 was also known as circ-Astn1. The entire mature spliced sequence length was 967 bp. The gene is on chromosome 1: 160432178-160441253 (Figure 2C).

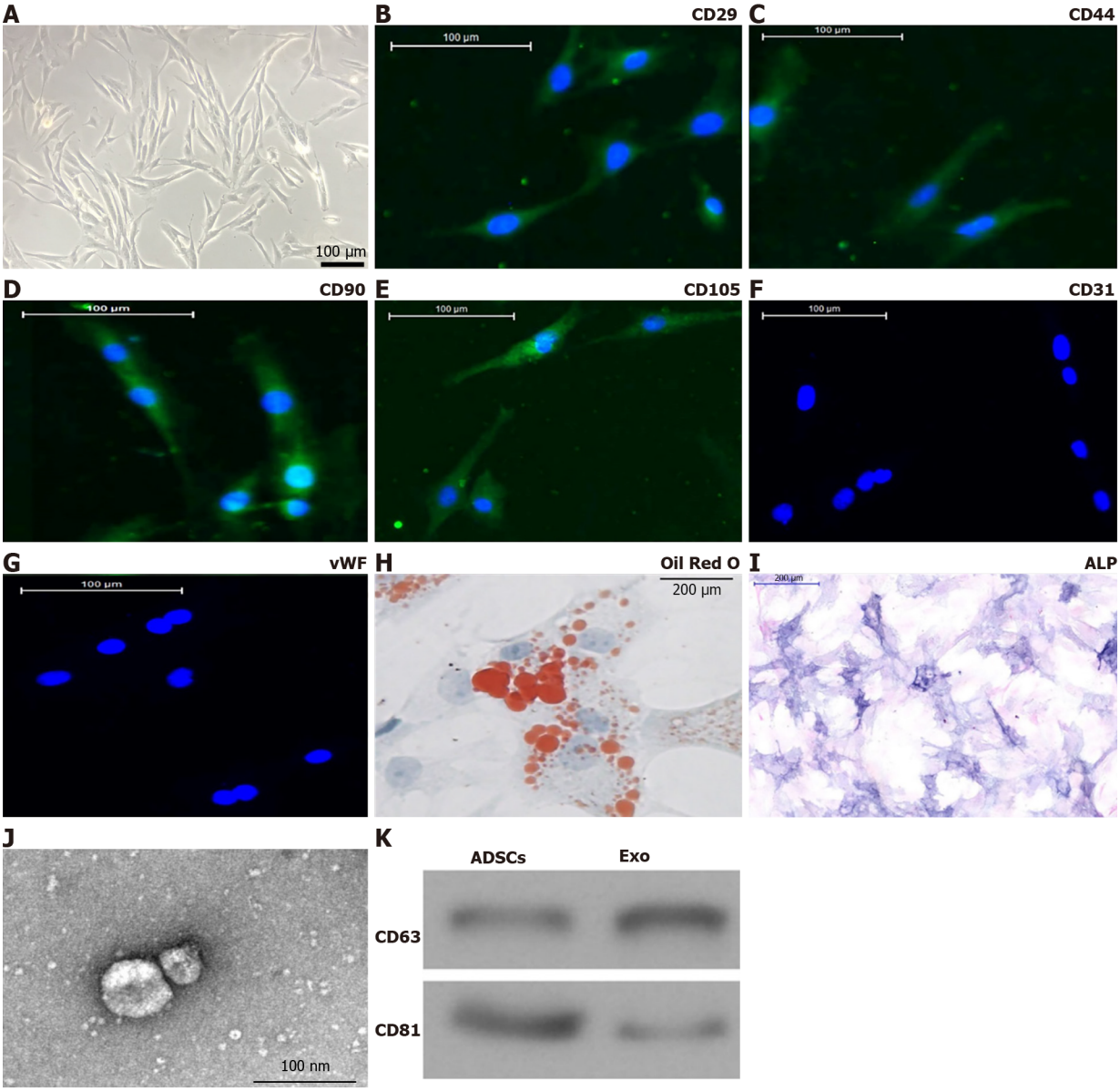

DOI: 10.4252/wjsc.v15.i5.476 **Copyright** ©The Author(s) 2023.

Figure 1 Characterization of adipose-derived mesenchymal stem cells and exosomes. A: Adipose-derived mesenchymal stem cells (ADSCs) showed a typical cobblestone-like morphology. Scale bar: 100 μm; B–G: Immunofluorescence staining of cell surface markers. ADSCs exhibited positive expression of cluster of differentiation 90 (CD90), CD29, CD44, and CD105, but not von Willebrand factor or CD34. Scale bar: 100 μm; H and I: The differentiation potential of ADSCs assessed by Oil Red O (H) and alkaline phosphatase (I) staining. Scale bar: 200 μm; J: Transmission electron micrographs demonstrated ADSC exosome morphology. Scale bar: 100 nm; K: Western blotting detection of CD81 and CD63 expression in exosomes and ADSCs.

Flow cytometry investigations have shown that HG (30 mmol/L glucose) treatment promotes EPC apoptosis. Treatment with Exos from WT ADSCs suppressed HG-induced EPC apoptosis, and treatment with Exos from ADSCs overexpressing circ-Astn1 had a more significant effect in suppressing HG-induced apoptosis of EPCs than Exos from WT ADSCs (Figure 2D and E), suggesting that circ-Astn1 played an important role in ADSC-Exo-mediated EPC protection under HG conditions. CCK8 detection confirmed that treatment with Exos containing high levels of circ-Astn1 had a greater effect in restoring the proliferative ability of EPCs under HG conditions (Figure 2F). We used tubule formation by EPCs in Matrigel-coated culture wells as an *in vitro* angiogenesis model, and evaluated their potential by counting the branch numbers formed. HG conditions suppressed angiogenesis, and treatment with Exos containing high levels of circ-Astn1 was more effective in promoting angiogenesis of EPCs under HG conditions (Figure 2G-J).

The circ-Astn1-mediated miR-138-5p/SIRT1/FOXO1 signaling pathway protects EPCs under HG conditions by promoting angiogenesis

Bioinformatics data showed that circ-Astn1 regulates SIRT1 expression *via* inhibition of miR-138-5p. SIRT1 functions critically in promoting angiogenesis by activating the FOXO1 signaling pathway[22]. To

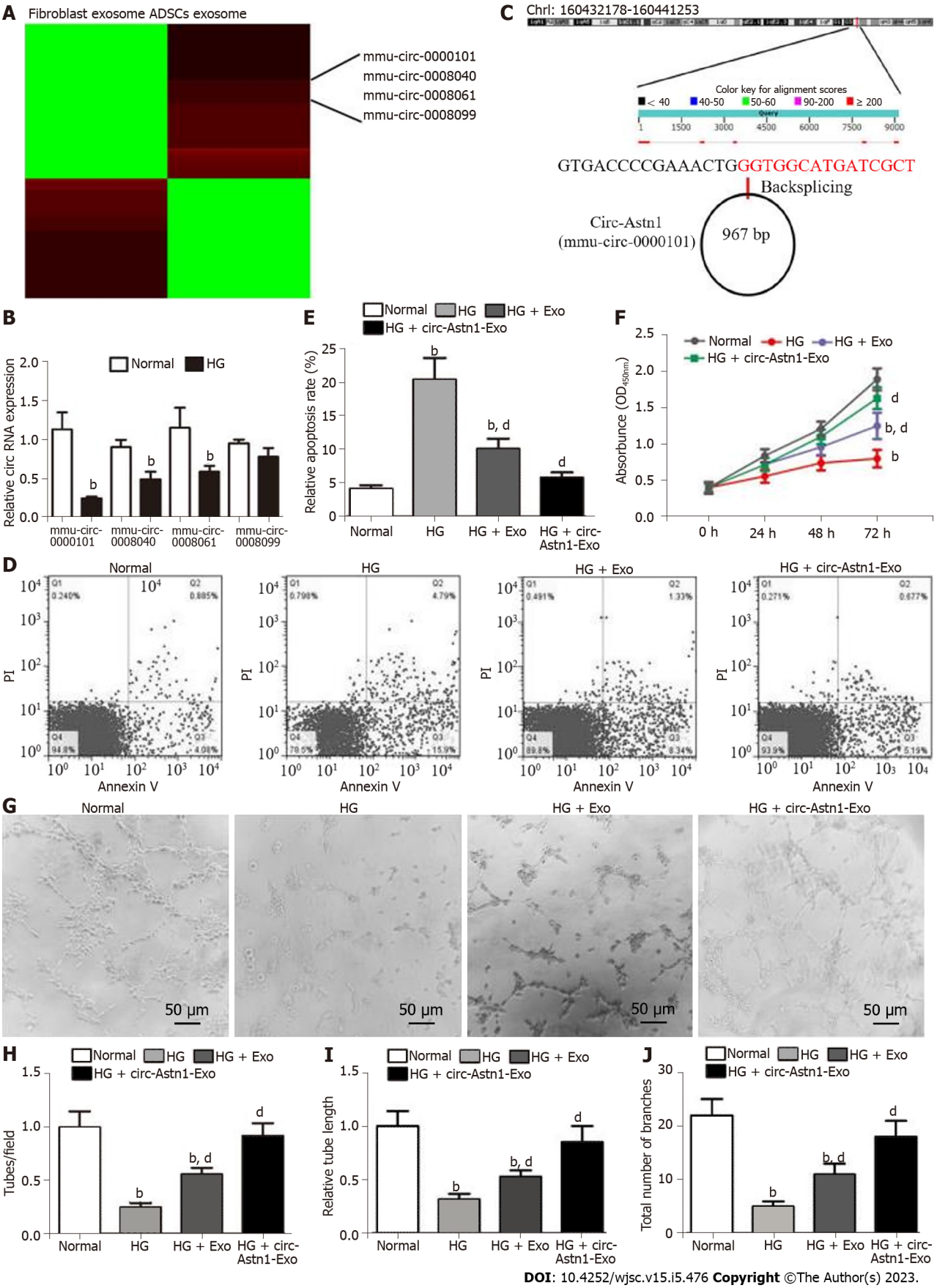

DOI: 10.4252/wjsc.v15.i5.476 **Copyright** ©The Author(s) 2023.

Figure 2 Exosomes derived from circular RNA astrotactin 1-modified adipose-derived mesenchymal stem cells function importantly in endothelial precursor cell function restoration by decreasing apoptosis under high glucose conditions. A: Heat map regarding all differentially expressed circular RNAs (circRNAs) between adipose-derived mesenchymal stem cells (ADSCs) exosomes and fibroblast exosomes; B: Quantitative polymerase chain reaction giving mmu_circ_0000101 (circular RNA astrotactin 1), mmu_circ_0008040, mmu_circ_0008061, and mmu_circ_0008099 expression in endothelial

precursor cells (EPCs) with or without high glucose (HG) treatment. Data are denoted by the mean ± SD; $^{b}P < 0.001$ *vs* normal; C: The genomic loci of circ-Astn1; D and E: We pretreated EPCs with ADSC exosomes before treatment with exosomes for 1 d under HG conditions. Our team assayed EPC apoptosis *via* flow cytometry after annexin V-FITC staining. $^{b}P < 0.001$ *vs* normal. $^{d}P < 0.001$ *vs* HG; F: EPC proliferation under different treatments, determined by Cell Counting Kit-8 assay. $^{b}P < 0.001$ *vs* normal. $^{d}P < 0.001$ *vs* HG; G-J: Representative photomicrographs of tube-like structures. Scale bar: 50 μm. Technician-counted tube branch points (H), relative tube length (I) and the total number of branches were calculated. $^{b}P < 0.001$ *vs* normal. $^{d}P < 0.001$ *vs* HG. PI: Propidium iodide.

validate the interaction among circ-Astn1, SIRT1, and miR-138-5p, we created a luciferase reporter (LR) vector. The candidate miR-138-5p-binding sites on circ-Astn1 as well as sites with point mutations inserted to prevent binding are shown in Figure 3A. Luciferase activity assay using 293T cells, which we transfected with MUT or WT circ-Astn1, verified that miR-138-5p suppressed circ-Astn1 activity (Figure 3B). RT-qPCR analysis suggested that circ-Astn1 overexpression suppressed miR-138-5p expression in EPCs (Figure 3C). Meanwhile the tubule formation assay showed that upregulation of circ-Astn1 restored angiogenic differentiation ability under HG conditions, but miR-138-5p overexpression destroyed the protective effect of circ-Astn1 (Figure 3D-G).

Next, we created the LR vector. Candidate miR-138-5p-binding sites on SIRT1 3'-UTR and those with point mutations inserted to prevent binding were constructed (Figure 3H). We transfected 293T cells with MUT or WT SIRT1 3'-UTR, which verified that WT miR-138-5p suppressed SIRT1 activity (Figure 3I). RT-qPCR analysis illustrated that miR-138-5p overexpression suppressed FOXO1 and SIRT1 expression at both mRNA and protein levels relating to EPCs (Figure 3J and K). However, overexpression of SIRT1 promoted SIRT1 and downregulated FOXO1 expression even after miR-138-5p overexpression. Analysis of tubule formation verified that miR-138-5p upregulation decreased angiogenic differentiation ability, but overexpression of SIRT1 restored the angiogenic differentiation ability of EPCs (Figure 3L-O).

Exos from circ-Astn1-modified ADSCs possess high therapeutic effect, enhancing wound healing

We investigated the influence of ADSC Exos on wound healing in full-thickness cutaneous wounds in mouse feet in a model of STZ-induced diabetes. Mice were treated by subcutaneous injection of Exos from WT or circ-Astn1-modified ADSCs, or an equivalent volume of PBS Exo diluent. Exos with high circ-Astn1 concentration accelerated wound closure significantly compared to PBS-treated control mice. The wounds treated with high circ-Astn1-containing Exos were almost closed by 14 d, while large areas of scarring were visible in both controls and circ-Astn1-knockdown-Exo-treated wounds (Figure 4A). Immunofluorescence with CD31 staining verified that microvascular development was more extensive with Exo treatments, specifically with high-circ-Astn1-containing Exos compared with the control group. However, circ-Astn1-knockdown suppressed the therapeutic effect of Exos (Figure 4B and C). TUNEL staining suggested that circ-Astn1 Exos significantly suppressed skin tissue apoptosis compared with control treatment, but circ-Astn1-knockdown suppressed the therapeutic effect of Exos (Figure 4D and E). Hematoxylin and eosin staining also showed that circ-Astn1 Exos treatment significantly promoted skin tissue wound healing compared with control treatment, but circ-Astn1-knockdown suppressed the therapeutic effect of Exos (Figure 4F). RT-qPCR analysis confirmed that circ-Astn1 Exos significantly suppressed miR-138-5p expression (Figure 4G) but promoted SIRT1 (Figure 4H) and decreased FOXO1 (Figure 4I) expression at both the mRNA and protein levels compared with controls.

DISCUSSION

Vascular deficits are fundamental factors regarding diabetes-related traits. Although former investigations have revealed that the proangiogenic wound healing phase is blunted by diabetes, detailed knowledge of factors regulating skin revascularization as well as capillary stabilization in diabetic wounds was missing[23]. Previous investigations revealed that Exos derived from ADSCs promote diabetic wound healing by regulating the disease microenvironment[4,20]. There is also evidence that circRNAs belong to a new RNA family that has been found to be broadly expressed, and have indispensable biological activities in regulating skin wound healing[18]. In this study, we found a series of circRNAs, which RNA-Seq detection showed were abnormally expressed in ADSC Exos compared with fibroblast Exos. Among the abnormally expressed circRNAs, expression of mmu_circ_0000101 (circ-Astn1), mmu_circ_0008040, mmu_circ_0008061, and mmu_circ_0008099 was all increased significantly in ADSC Exos. Further study showed that circ-Astn1 decreased more significantly in EPCs after exposure to HG conditions. This suggesting that ADSC Exos protected EPCs from HG-induced damage related to circ-Astn1 delivery.

Our *in vitro* experiments revealed that HG conditions promoted EPC apoptosis and destroyed the ability of EPCs to differentiate into blood vessels. Transplantation of ADSC Exos exerted a protective effect in reversing HG-induced EPC damage. Increasing the circ-Astn1 content of Exos increased the protective effect. Bioinformatics analyses identified miR-138-5p as the circ-Astn1 downstream target, and this was confirmed by luciferase reporter (LR) experiments. A previous study revealed that overex-

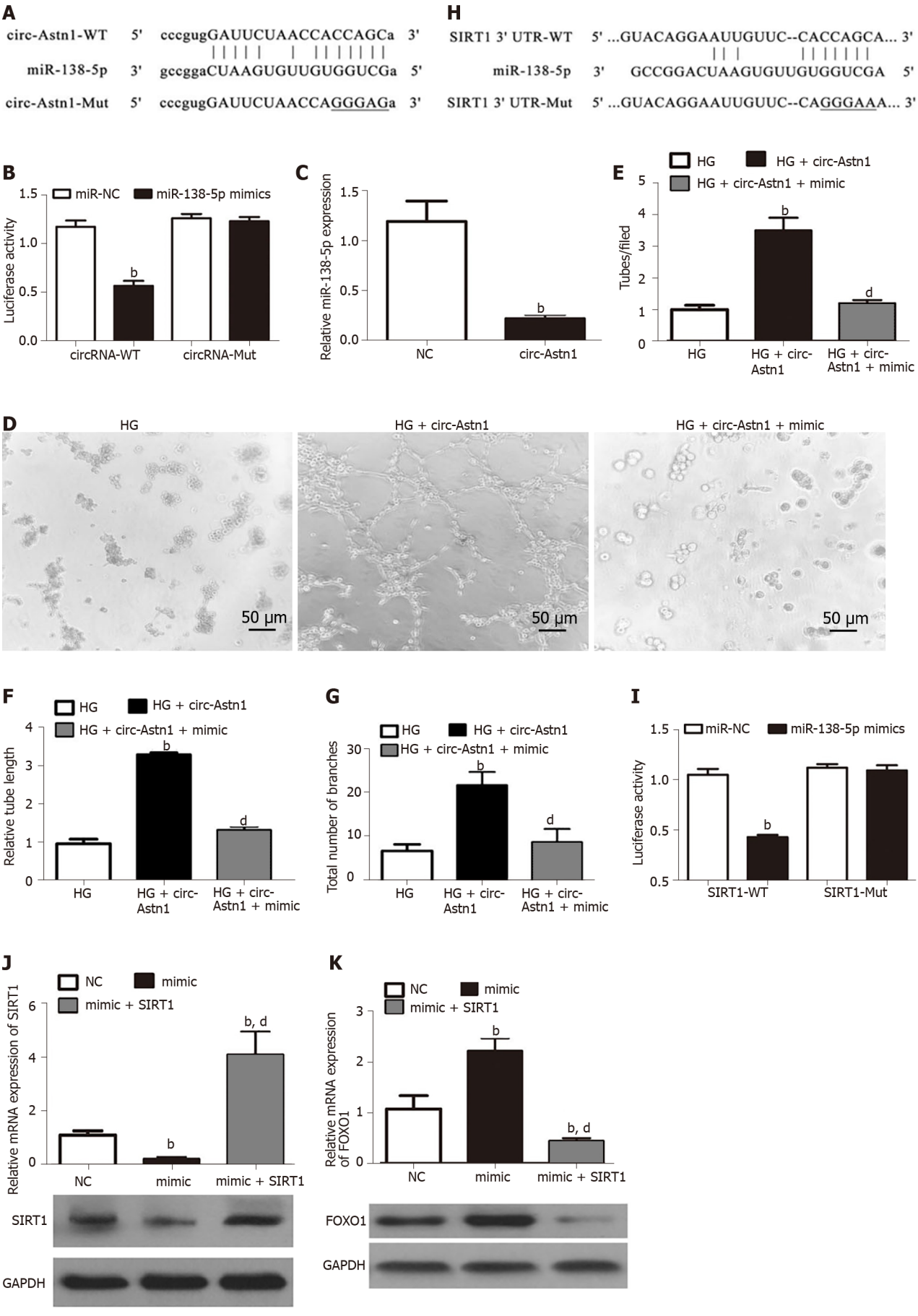
A
circ-Astn1-WT 5' cccgugGAUUCUAACCACCAGCa 3'
miR-138-5p 3' gccggaCUAAGUGUUGUGGUCGa 5'
circ-Astn1-Mut 5' cccgugGAUUCUAACCAGGGAGa 3'
H
SIRT1 3' UTR-WT 5' ...GUACAGGAAUUGUUC--CACCAGCA... 3'
miR-138-5p 3' GCCGGACUAAGUGUUGUGGUCGA 5'
SIRT1 3' UTR-Mut 5' ...GUACAGGAAUUGUUC--CAGGGAAA... 3'
B
miR-NC
miR-138-5p mimics
Luciferase activity
circRNA-WT
circRNA-Mut
C
Relative miR-138-5p expression
NC
circ-Astn1
E
HG
HG + circ-Astn1
HG + circ-Astn1 + mimic
Tubes/filed
D
HG
HG + circ-Astn1
HG + circ-Astn1 + mimic
50 μm
F
Relative tube length
G
Total number of branches
I
SIRT1-WT
SIRT1-Mut
J
NC
mimic
mimic + SIRT1
Relative mRNA expression of SIRT1
SIRT1
GAPDH
K
Relative mRNA expression of FOXO1
FOXO1
GAPDH

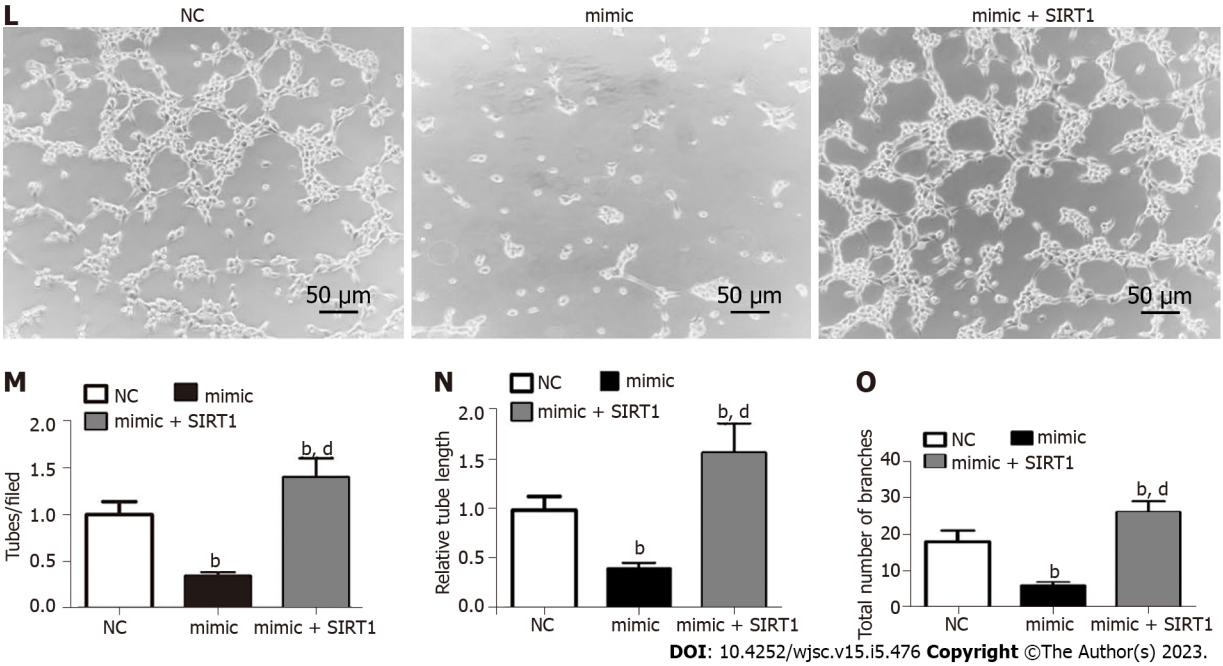

DOI: 10.4252/wjsc.v15.i5.476

Figure 3 The circular RNA astrotactin 1-mediated mi-138-5p/SIRT1/forkhead box O1 signaling pathway plays an important protective role in endothelial precursor cells under high glucose conditions by promoting angiogenesis. A and B: Luciferase expression levels in HEK293 cells transfected with cloned circular RNA astrotactin 1 (circ-Astn1) wild-type (WT) or mutant (MUT) vector and miR-138-5p mimics. Data are denoted by the mean ± SD. $^{b}P < 0.001$; C: Quantitative polymerase chain reaction (qPCR) detection suggested that miR-138-5p expression was reduced after transfection with circ-Astn1-overexpressing vector in endothelial precursor cells (EPCs). Data are denoted as the mean ± SD. $^{b}P < 0.001$ *vs* NC; D-G: Representative photomicrographs of tube-like structures of EPCs under high glucose (HG) conditions after transfection with negative control or circ-Astn1-overexpressing vector. $^{b}P < 0.001$ *vs* HG. $^{d}P < 0.001$ *vs* circ-Astn1; H and I: Luciferase expression level in HEK293 cells transfected with cloned SIRT1 WT- or MUT-3' UTR vector and miR-138-5p mimics. Data are denoted by the mean ± SD. $^{b}P < 0.001$; J and K: qPCR and western blot analysis indicated that SIRT1 and forkhead box O1 expression were reduced after transfection with miR-138-5p overexpression vector in EPCs. Data are expressed as the mean ± SD. $^{b}P < 0.001$ *vs* NC. $^{d}P < 0.001$ *vs* miR-138-5p mimics; L-O: Representative photomicrographs of EPC tube-like structures under HG conditions after transfection with miR-138-5p mimics combined with or without SIRT1 overexpression vector. Data are denoted by the mean ± SD. $^{b}P < 0.001$ *vs* NC. $^{d}P < 0.001$ *vs* miR-138-5p mimics.

pression of miR-138 aggravates HG-induced vascular cell damage[24]. Our current investigation also found that circ-Astn1 overexpression decreased miR-138-5p expression. Meanwhile miR-138-5p overexpression reduced vascular EPC differentiation, suggesting that circ-Astn1 protected against HG-induced EPC damage by miR-138-5p adsorption.

Additional bioinformatics results showed that SIRT1 was also a miR-138-5p downstream target and this was verified by LR experiments. SIRT1 is a highly conserved nicotinamide adenosine dinucleotide (NAD)-dependent deacetylase, which plays a regulatory role in metabolism and aging[25]. miR-138-5p overexpression reduced SIRT1 expression. Overexpression of SIRT1 restored vascular differentiation of EPCs after miR-138-5p upregulation. Previous studies have suggested that the SIRT1/FOXO1 pathway activity improves the stress microenvironment[26-28]. SIRT1 correlates to and deacetylates FoxO1. Moreover, previous studies have confirmed that SIRT1, a deacetylase that suppresses FoxO1 acetylation which is a crucial negative blood vessel development regulator, restrains anti-angiogenic activity[22,29,30]. Recently, it was reported that oxidative stress induces FoxO1 nuclear translocation which plays an important role in apoptosis regulation[26]. *In vivo* experiments have confirmed that Exos originating from circ-Astn1-modified ADSCs function indispensably in restoring EPC function and promoting wound healing by promotion of angiogenesis and suppression of apoptosis. RT-qPCR analysis demonstrated that treatment with Exos containing high levels of circ-Astn1 reduced miR-138-5p expression and promoted SIRT1. This increase in SIRT1 level suppressed FOXO1 expression, suggesting that Exos derived from circ-Astn1-modified ADSCs enhanced wound healing in a diabetic mouse model *via* miR-138-5p/SIRT1/FOXO1 axis regulation.

CONCLUSION

In conclusion, our research indicated that Exos derived from circ-Astn1-modified ADSCs enhanced wound healing in a diabetic mouse model *via* miR-138-5p/SIRT1/FOXO1 axis induction. Our study verified the therapeutic effects of circ-Astn1-Exos on an STZ-induced diabetic wound healing model. However, more in-depth studies are required to determine the actual role of miR-138-5p/SIRT1/FOXO1 in wound healing.

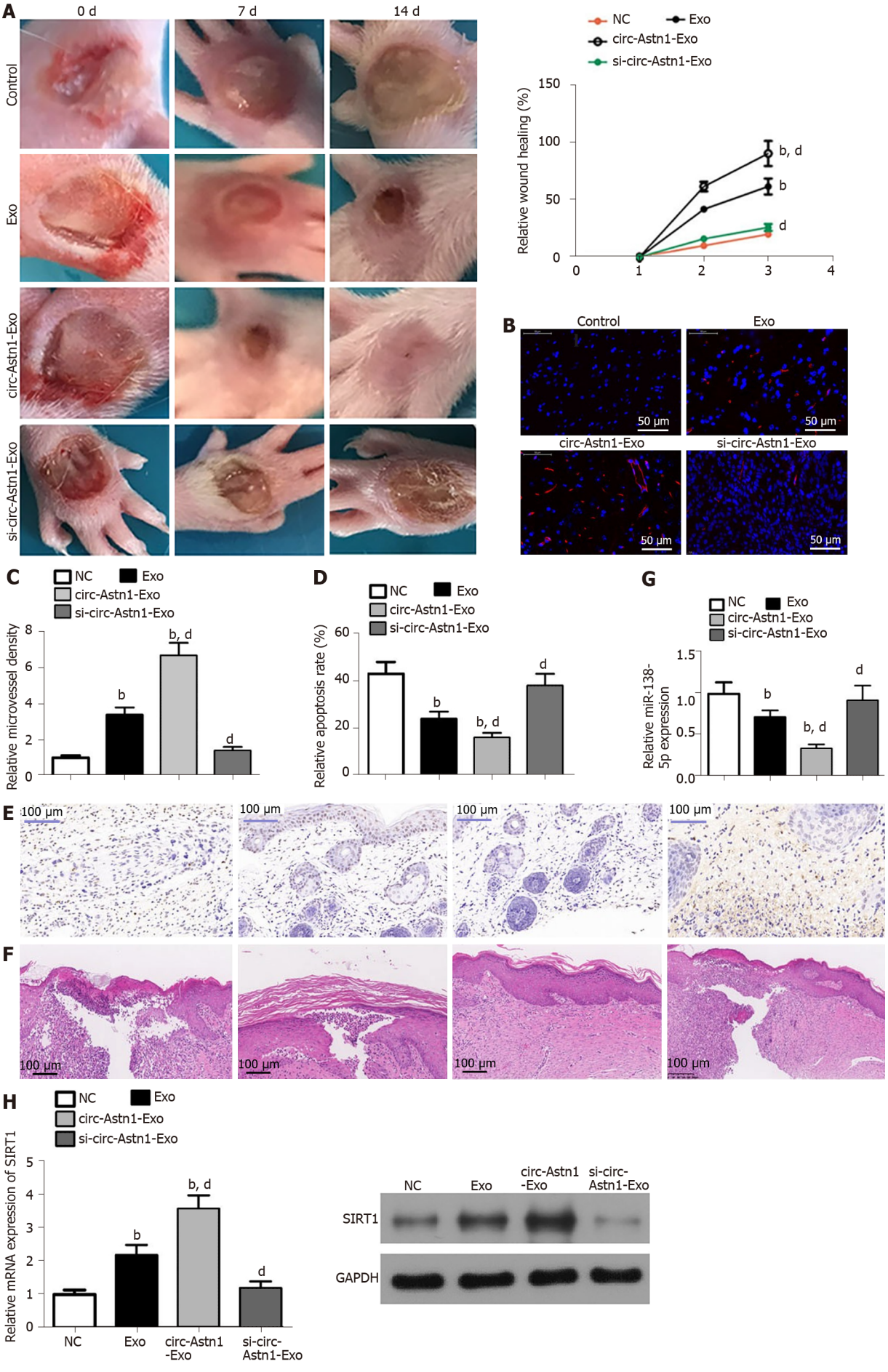
A
0 d
7 d
14 d
Control
Exo
circ-Astn1-Exo
si-circ-Astn1-Exo
NC
Exo
circ-Astn1-Exo
si-circ-Astn1-Exo
Relative wound healing (%)
150
100
50
0
0
1
2
3
4
b, d
b
d
B
Control
Exo
circ-Astn1-Exo
si-circ-Astn1-Exo
50 μm
C
NC
Exo
circ-Astn1-Exo
si-circ-Astn1-Exo
Relative microvessel density
8
6
4
2
0
b
b, d
d
D
NC
Exo
circ-Astn1-Exo
si-circ-Astn1-Exo
Relative apoptosis rate (%)
60
40
20
0
b
b, d
d
G
NC
Exo
circ-Astn1-Exo
si-circ-Astn1-Exo
Relative miR-138-5p expression
1.5
1.0
0.5
0.0
b
b, d
d
E
100 μm
F
100 μm
H
NC
Exo
circ-Astn1-Exo
si-circ-Astn1-Exo
Relative mRNA expression of SIRT1
5
4
3
2
1
0
b
b, d
d
NC
Exo
circ-Astn1-Exo
si-circ-Astn1-Exo
SIRT1
GAPDH

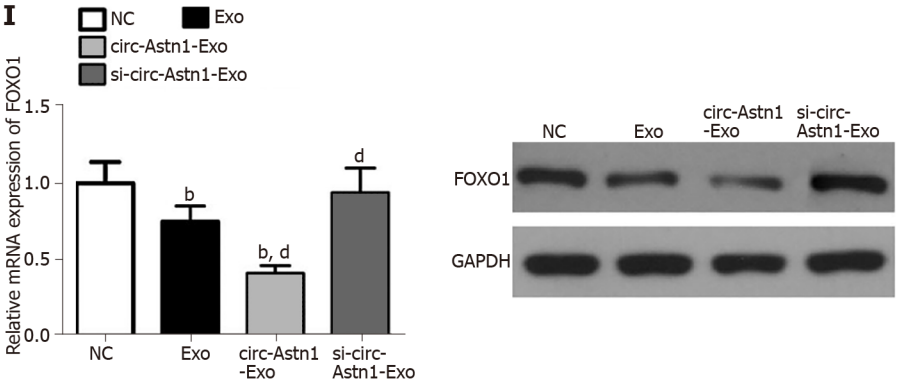

DOI: 10.4252/wjsc.v15.i5.476 **Copyright** ©The Author(s) 2023.

Figure 4 Exosomes from circular RNA astrotactin 1-modified adipose-derived mesenchymal stem cells have greater therapeutic effect in promoting wound healing in a diabetic mouse model. A: Representative images of full-thickness skin defects after treatment with adipose-derived mesenchymal stem cell (ADSC) exosomes or circular RNA astrotactin 1-modified ADSC exosomes for 0, 1, and 2 wk after wounding; B and C: Microvascular formation evaluated by immunofluorescence staining with cluster of differentiation 31. $^{b}P < 0.001$ *vs* control. $^{d}P < 0.001$ *vs* exosomes; D and E: We assayed apoptosis level *via* terminal deoxynucleotidyl transferase dUTP nick end labeling staining. $^{b}P < 0.001$ *vs* control. $^{d}P < 0.001$ *vs* exosomes; F: Hematoxylin and eosin staining shows wound changes; G-I: Quantitative polymerase chain reaction and western blot analysis showing mi-138-5p (G), SIRT1 (H), and forkhead box O1 (I) expression. $^{b}P < 0.001$ *vs* control. $^{d}P < 0.001$ *vs* exosomes.

ARTICLE HIGHLIGHTS

Research background

Wound healing impairment is a dysfunction induced by hyperglycemia and its effect on endothelial precursor cells (EPCs) in type 2 diabetes mellitus. There is increasing evidence showing that exosomes (Exos) derived from adipose-derived mesenchymal stem cells (ADSCs) exhibit the potential to improve endothelial cell function along with the wound healing process.

Research motivation

The potential therapeutic mechanism of ADSC Exos in wound healing in diabetic mice remains unclear.

Research objectives

To verify the effect of treatment with Exos from circular RNA astrotactin 1 (circ-Astn1)-overexpressing ADSCs on high glucose (HG)-induced EPC dysfunction.

Research methods

In this study, Exos from ADSCs and fibroblasts were used for high-throughput RNA sequencing (RNA-Seq). ADSC-Exo-mediated healing of full-thickness skin wounds in a diabetic mouse model was investigated. We utilized EPCs to investigate the therapeutic function of Exos in cell damage and dysfunction caused by HG. We utilized a luciferase reporter (LR) assay to detect interactions among circ-Astn1, SIRT1 and miR-138-5p. We employed diabetic mice to verify the therapeutic effect of circ-Astn1 on Exo-mediated wound healing.

Research results

High-throughput RNA-Seq detection showed that circ-Astn1 expression was increased in ADSC Exos compared with Exos from fibroblasts. Exos containing high concentrations of circ-Astn1 had enhanced therapeutic effect in restoring EPC function under HG conditions by promoting SIRT1 expression. Circ-Astn1 expression enhanced SIRT1 expression through miR-138-5p adsorption, which was validated by LR assay along with bioinformatics analyses. Exos containing high concentrations of circ-Astn1 had better therapeutic effect on wound healing *in vivo* compared to wild-type ADSC Exos. Immunofluorescence and immunohistochemical investigations suggested that circ-Astn1 enhanced angiopoiesis through Exo treatment of wounded skin as well as suppressing apoptosis through promotion of SIRT1 and decreased FOXO1 expression.

Research conclusions

In summary, we concluded that circ-Astn1 promoted the therapeutic effect of ADSC-Exos and thus improved wound healing in diabetes *via* miR-138-5p absorption and SIRT1 upregulation. Based on our data, we advocate targeting the circ-Astn1/miR-138-5p/SIRT1 axis as a potential therapeutic alternative for treatment of diabetic ulcers.

Research perspectives

More in-depth studies are required to determine the actual role of miR-138-5p/SIRT1/FOXO1 in wound healing.

FOOTNOTES

Author contributions: Wang Z and Wang YB designed the project and drafted the paper based on feedback from the other authors; Feng C, Liu H, and Meng T performed all experiments and analyses; Huang WQ and Song KX took part in the analyses and draft revision.

Supported by The Beijing Municipal Natural Science Foundation, No. 7192160.

Institutional animal care and use committee statement: The Animal Care and Use Committee of Peking Union Medical College Hospital approved the investigation protocol (No: XHDW-2020-01). We carried out all postoperative animal care along with surgical interventions following the NIH Guide for Care and Use of Laboratory Animals. All surgery and euthanasia were performed under sodium pentobarbital anesthesia (30 mg/kg) by intraperitoneal injection, and all efforts were made to minimize suffering.

Conflict-of-interest statement: The authors have no conflicts of interest to declare.

Data sharing statement: The datasets used or/and analyzed during the current study are available from the corresponding author on reasonable request.

ARRIVE guidelines statement: The authors have read the ARRIVE Guidelines, and the manuscript was prepared and revised according to the ARRIVE Guidelines.

Country/Territory of origin: China

ORCID number: Zhi Wang 0000-0001-6116-2992; Cheng Feng 0000-0001-5603-5681; Hao Liu 0000-0003-0423-6304; Tian Meng 0000-0003-1289-0031; Wei-Qing Huang 0000-0002-2123-8830; Ke-Xin Song 0000-0003-4614-589X; You-Bin Wang 0000-0001-5373-2633.

S-Editor: Fan JR
L-Editor: Filipodia
P-Editor: Yu HG

REFERENCES

1 **Lehrman JD**. Combining the Benefits of Collagen and Negative Pressure Wound Therapy to Heal a Chronic Diabetic Foot Ulcer: A Case Report. *Wounds* 2020; **32**: E11-E13 [PMID: 32335522]
2 **Al-Shamsi M**, Amin A, Adeghate E. Vitamin E ameliorates some biochemical parameters in normal and diabetic rats. *Ann N Y Acad Sci* 2006; **1084**: 411-431 [PMID: 17151319 DOI: 10.1196/annals.1372.033]
3 **Al-Shamsi M**, Amin A, Adeghate E. Effect of vitamin C on liver and kidney functions in normal and diabetic rats. *Ann N Y Acad Sci* 2006; **1084**: 371-390 [PMID: 17151316 DOI: 10.1196/annals.1372.031]
4 **Li X**, Xie X, Lian W, Shi R, Han S, Zhang H, Lu L, Li M. Exosomes from adipose-derived stem cells overexpressing Nrf2 accelerate cutaneous wound healing by promoting vascularization in a diabetic foot ulcer rat model. *Exp Mol Med* 2018; **50**: 1-14 [PMID: 29651102 DOI: 10.1038/s12276-018-0058-5]
5 **Li G**, Peng H, Qian S, Zou X, Du Y, Wang Z, Zou L, Feng Z, Zhang J, Zhu Y, Liang H, Li B. Bone Marrow-Derived Mesenchymal Stem Cells Restored High-Fat-Fed Induced Hyperinsulinemia in Rats at Early Stage of Type 2 Diabetes Mellitus. *Cell Transplant* 2020; **29**: 963689720904628 [PMID: 32228047 DOI: 10.1177/0963689720904628]
6 **Gorecka J**, Gao X, Fereydooni A, Dash BC, Luo J, Lee SR, Taniguchi R, Hsia HC, Qyang Y, Dardik A. Induced pluripotent stem cell-derived smooth muscle cells increase angiogenesis and accelerate diabetic wound healing. *Regen Med* 2020; **15**: 1277-1293 [PMID: 32228292 DOI: 10.2217/rme-2019-0086]
7 **An R**, Zhang Y, Qiao Y, Song L, Wang H, Dong X. Adipose stem cells isolated from diabetic mice improve cutaneous wound healing in streptozotocin-induced diabetic mice. *Stem Cell Res Ther* 2020; **11**: 120 [PMID: 32183899 DOI: 10.1186/s13287-020-01621-x]
8 **Ding J**, Wang X, Chen B, Zhang J, Xu J. Exosomes Derived from Human Bone Marrow Mesenchymal Stem Cells Stimulated by Deferoxamine Accelerate Cutaneous Wound Healing by Promoting Angiogenesis. *Biomed Res Int* 2019;

2019: 9742765 [PMID: 31192260 DOI: 10.1155/2019/9742765]

9 **Leszczynska A**, Kulkarni M, Ljubimov AV, Saghizadeh M. Exosomes from normal and diabetic human corneolimbal keratocytes differentially regulate migration, proliferation and marker expression of limbal epithelial cells. *Sci Rep* 2018; **8**: 15173 [PMID: 30310159 DOI: 10.1038/s41598-018-33169-5]

10 **Shi Q**, Qian Z, Liu D, Sun J, Wang X, Liu H, Xu J, Guo X. GMSC-Derived Exosomes Combined with a Chitosan/Silk Hydrogel Sponge Accelerates Wound Healing in a Diabetic Rat Skin Defect Model. *Front Physiol* 2017; **8**: 904 [PMID: 29163228 DOI: 10.3389/fphys.2017.00904]

11 **Guo SC**, Tao SC, Yin WJ, Qi X, Yuan T, Zhang CQ. Exosomes derived from platelet-rich plasma promote the re-epithelization of chronic cutaneous wounds *via* activation of YAP in a diabetic rat model. *Theranostics* 2017; **7**: 81-96 [PMID: 28042318 DOI: 10.7150/thno.16803]

12 **Hu JL**, Wang W, Lan XL, Zeng ZC, Liang YS, Yan YR, Song FY, Wang FF, Zhu XH, Liao WJ, Liao WT, Ding YQ, Liang L. CAFs secreted exosomes promote metastasis and chemotherapy resistance by enhancing cell stemness and epithelial-mesenchymal transition in colorectal cancer. *Mol Cancer* 2019; **18**: 91 [PMID: 31064356 DOI: 10.1186/s12943-019-1019-x]

13 **Jiang J**, Li J, Zhou X, Zhao X, Huang B, Qin Y. Exosomes Regulate the Epithelial-Mesenchymal Transition in Cancer. *Front Oncol* 2022; **12**: 864980 [PMID: 35359397 DOI: 10.3389/fonc.2022.864980]

14 **Jin J**, Shi Y, Gong J, Zhao L, Li Y, He Q, Huang H. Exosome secreted from adipose-derived stem cells attenuates diabetic nephropathy by promoting autophagy flux and inhibiting apoptosis in podocyte. *Stem Cell Res Ther* 2019; **10**: 95 [PMID: 30876481 DOI: 10.1186/s13287-019-1177-1]

15 **Qiu J**, Shu C, Li X, Ye C, Zhang WC. Exosomes from linc00511-overexpressing ADSCs accelerates angiogenesis in diabetic foot ulcers healing by suppressing PAQR3-induced Twist1 degradation. *Diabetes Res Clin Pract* 2021; **180**: 109032 [PMID: 34461141 DOI: 10.1016/j.diabres.2021.109032]

16 **Xia L**, Song M. Role of Non-coding RNA in Diabetic Cardiomyopathy. *Adv Exp Med Biol* 2020; **1229**: 181-195 [PMID: 32285412 DOI: 10.1007/978-981-15-1671-9_10]

17 **He M**, Wang W, Yu H, Wang D, Cao D, Zeng Y, Wu Q, Zhong P, Cheng Z, Hu Y, Zhang L. Comparison of expression profiling of circular RNAs in vitreous humour between diabetic retinopathy and non-diabetes mellitus patients. *Acta Diabetol* 2020; **57**: 479-489 [PMID: 31749049 DOI: 10.1007/s00592-019-01448-w]

18 **Wang A**, Toma MA, Ma J, Li D, Vij M, Chu T, Wang J, Li X, Xu Landén N. Circular RNA hsa_circ_0084443 Is Upregulated in Diabetic Foot Ulcer and Modulates Keratinocyte Migration and Proliferation. *Adv Wound Care (New Rochelle)* 2020; **9**: 145-160 [PMID: 32117579 DOI: 10.1089/wound.2019.0956]

19 **Zhu K**, Hu X, Chen H, Li F, Yin N, Liu AL, Shan K, Qin YW, Huang X, Chang Q, Xu GZ, Wang Z. Downregulation of circRNA DMNT3B contributes to diabetic retinal vascular dysfunction through targeting miR-20b-5p and BAMBI. *EBioMedicine* 2019; **49**: 341-353 [PMID: 31636010 DOI: 10.1016/j.ebiom.2019.10.004]

20 **Shi R**, Jin Y, Hu W, Lian W, Cao C, Han S, Zhao S, Yuan H, Yang X, Shi J, Zhao H. Exosomes derived from mmu_circ_0000250-modified adipose-derived mesenchymal stem cells promote wound healing in diabetic mice by inducing miR-128-3p/SIRT1-mediated autophagy. *Am J Physiol Cell Physiol* 2020; **318**: C848-C856 [PMID: 32159361 DOI: 10.1152/ajpcell.00041.2020]

21 **Li R**, Chen C, Zheng RQ, Zou L, Hao GL, Zhang GC. Influences of hucMSC-exosomes on VEGF and BMP-2 expression in SNFH rats. *Eur Rev Med Pharmacol Sci* 2019; **23**: 2935-2943 [PMID: 31002144 DOI: 10.26355/eurrev_201904_17573]

22 **Huang X**, Sun J, Chen G, Niu C, Wang Y, Zhao C, Huang H, Huang S, Liang Y, Shen Y, Cong W, Jin L, Zhu Z. Resveratrol Promotes Diabetic Wound Healing *via* SIRT1-FOXO1-c-Myc Signaling Pathway-Mediated Angiogenesis. *Front Pharmacol* 2019; **10**: 421 [PMID: 31068817 DOI: 10.3389/fphar.2019.00421]

23 **Okonkwo UA**, Chen L, Ma D, Haywood VA, Barakat M, Urao N, DiPietro LA. Compromised angiogenesis and vascular Integrity in impaired diabetic wound healing. *PLoS One* 2020; **15**: e0231962 [PMID: 32324828 DOI: 10.1371/journal.pone.0231962]

24 **Qian C**, Liang S, Wan G, Dong Y, Lu T, Yan P. Salidroside alleviates high-glucose-induced injury in retinal pigment epithelial cell line ARPE-19 by down-regulation of miR-138. *RNA Biol* 2019; **16**: 1461-1470 [PMID: 31251107 DOI: 10.1080/15476286.2019.1637696]

25 **Ren BC**, Zhang YF, Liu SS, Cheng XJ, Yang X, Cui XG, Zhao XR, Zhao H, Hao MF, Li MD, Tie YY, Qu L, Li XY. Curcumin alleviates oxidative stress and inhibits apoptosis in diabetic cardiomyopathy *via* Sirt1-Foxo1 and PI3K-Akt signalling pathways. *J Cell Mol Med* 2020; **24**: 12355-12367 [PMID: 32961025 DOI: 10.1111/jcmm.15725]

26 **Yan X**, Yu A, Zheng H, Wang S, He Y, Wang L. Calycosin-7-*O*-*β*-*D*-glucoside Attenuates OGD/R-Induced Damage by Preventing Oxidative Stress and Neuronal Apoptosis *via* the SIRT1/FOXO1/PGC-1*α* Pathway in HT22 Cells. *Neural Plast* 2019; **2019**: 8798069 [PMID: 31885537 DOI: 10.1155/2019/8798069]

27 **Al-Massadi O**, Quiñones M, Clasadonte J, Hernandez-Bautista R, Romero-Picó A, Folgueira C, Morgan DA, Kalló I, Heras V, Senra A, Funderburk SC, Krashes MJ, Souto Y, Fidalgo M, Luquet S, Chee MJ, Imbernon M, Beiroa D, García-Caballero L, Gallego R, Lam BYH, Yeo G, Lopez M, Liposits Z, Rahmouni K, Prevot V, Dieguez C, Nogueiras R. MCH Regulates SIRT1/FoxO1 and Reduces POMC Neuronal Activity to Induce Hyperphagia, Adiposity, and Glucose Intolerance. *Diabetes* 2019; **68**: 2210-2222 [PMID: 31530579 DOI: 10.2337/db19-0029]

28 **Sun DW**, Gao Q, Qi X. Danshensu Ameliorates Cardiac Ischaemia Reperfusion Injury through Activating Sirt1/FoxO1/Rab7 Signal Pathway. *Chin J Integr Med* 2020; **26**: 283-291 [PMID: 31254156 DOI: 10.1007/s11655-019-3165-9]

29 **Potente M**, Ghaeni L, Baldessari D, Mostoslavsky R, Rossig L, Dequiedt F, Haendeler J, Mione M, Dejana E, Alt FW, Zeiher AM, Dimmeler S. SIRT1 controls endothelial angiogenic functions during vascular growth. *Genes Dev* 2007; **21**: 2644-2658 [PMID: 17938244 DOI: 10.1101/gad.435107]

30 **Tie L**, An Y, Han J, Xiao Y, Xiaokaiti Y, Fan S, Liu S, Chen AF, Li X. Genistein accelerates refractory wound healing by suppressing superoxide and FoxO1/iNOS pathway in type 1 diabetes. *J Nutr Biochem* 2013; **24**: 88-96 [PMID: 22819564 DOI: 10.1016/j.jnutbio.2012.02.011]

Published by **Baishideng Publishing Group Inc**
7041 Koll Center Parkway, Suite 160, Pleasanton, CA 94566, USA
Telephone: +1-925-3991568
E-mail: bpgoffice@wjgnet.com
Help Desk: https://www.f6publishing.com/helpdesk
https://www.wjgnet.com